scientific reports

Check for updates

OPEN

Asynchronous transfer of magmas and mineralizing fluids in a plutonic-subvolcanic-volcanic plumbing system

Gabriele Paoli[1,2]✉, Andrea Dini[3], Simone Vezzoni[3]✉, Maria Ovtcharova[4] & Sergio Rocchi[1,2]

The geochronological-geochemical interplay between magma transfer and mineralizing fluid is studied at Campiglia igneous complex, Tuscany. Here, crustal and mantle-derived magmas were emplaced at plutonic, subvolcanic, and volcanic level (5.4 to 4.4 Ma), and were quickly exhumed, thus allowing U–Pb CA-ID-TIMS zircon dating with error of ka to tens of ka. The igneous activity is intertwined with the genesis of Cu–Pb–Zn(–Ag) skarn deposits. A two-cycle scenario is reconstructed. In the first cycle, a bimodal deep magma reservoir remained in melt-present condition for ~ 500 ka. In this time interval, a peraluminous pluton is emplaced, followed by generation of distal skarn with related Zn–Pb(–Ag) sulfide ore. Later on, Fe–Cu ore is generated in association with mantle-derived mafic melts, and a peraluminous rhyolite eruption terminates the cycle. These crust- or mantle-derived igneous units show limited evidence for interaction. Early-crystallized, antecrystic zircons were recycled within portions of melts sequentially extracted from the reservoir. In the second cycle, during the following 500 ka, an independent reservoir freshly fed by interacting crustal and mantle melts gave eventually way to eruption of a hybrid rhyolite. Timescales of the Campiglia complex reveal significant asynchrony between magma feeding of the plutonic-subvolcanic-volcanic plumbing system and the mineralizing activity of igneous fluids.

Timescales are key to understanding the genetic link between plutonic and volcanic realms in igneous plumbing systems. High-precision zircon geochronology by CA-ID-TIMS (chemical abrasion isotope dilution thermal ionization mass spectrometry) is pivotal in estimating timescales for magma extraction, emplacement, and fluxes[1–3]. Zircon geochronology supports the idea of prolonged periods of zircon crystallization in felsic magmas[4–6]. Intrusive bodies can show cumulative time intervals of zircon crystallization significantly longer than the time required for the complete solidification of a single pulse of magma, suggesting a multistage, pulsed, growth history[7]. Moreover, zircon grains found in subvolcanic and volcanic bodies can originate in and be withdrawn from partly crystallized magma mushes before or during an eruption[8,9], either as isolated crystals or in mobilized residual melt pockets[10], thus providing key information on otherwise inaccessible portions of igneous systems[1]. Finally, combining timescales of events with petrological and isotopic data contributes to resolve the duration of processes at different levels of the plumbing system[11] as well as the nature of magma source(s)[12–14].

Timescale issues have been successfully addressed for rhyolite eruptions in volcanic arcs, deriving from either large-volume silicic magmas evolving as open systems assimilating older crust, or extended crystal fractionation at mid- to upper-crustal level of mantle-derived magmas[6,15–17]. Recently, timescales of such systems have also been proven as critical clues for the understanding of the interplay between magmatic and hydrothermal processes in the generation of porphyry-related ore deposits in subduction systems[18–20].

On the other hand, igneous plumbing systems fed by post-collisional crustal and mantle magmas and related to ore deposits are receiving comparatively little attention in terms of their timescale evolution, and even less for their relationships with magmatic-to-hydrothermal ore deposits. To contribute to fill this gap, we investigated the Miocene-Pliocene Campiglia Marittima igneous complex, Tuscany[21]. This complex is in many respects a unique example of a plumbing system where (i) crustal and mantle magmas did interact to generate a complete range of crustal, mantle and hybrid magmas, (ii) these magmas were emplaced at plutonic, subvolcanic, and volcanic levels over a time span of c. 1 Ma, (iii) a quick exhumation of the intrusive bodies occurred here[22], thus

[1]Dipartimento di Scienze Della Terra, Università di Pisa, Pisa, Italy. [2]Center for Instrument Sharing of the University of Pisa, CISUP, Pisa, Italy. [3]Istituto di Geoscienze e Georisorse, CNR, Pisa, Italy. [4]Department of Earth Sciences, University of Geneva, Geneva, Switzerland. ✉email: gabriele.paoli@unipi.it; simone.vezzoni@igg.cnr.it

exposing young plutonic and subvolcanic rocks as well as to their volcanic counterpart, and (iv) skarn and ore genesis occurred amidst magma emplacement/eruption events. These peculiar geological features combined with high-precision U–Pb CA-ID-TIMS zircon dating unveil processes internal to the plumbing system such as magma recharge-interaction in prolonged melt-present conditions, and zircon cannibalism by younger magma batches at the expense of older ones. Finally, the interleaving of igneous events with skarn/ore formation opens a window on the understanding of the link between magmatism, activity of mineralizing fluid and their timing and timescales, revealing an asynchrony between feeding processes and magma emplacement/eruption.

The Campiglia igneous complex

The Miocene-Quaternary Tuscan Magmatic Province (TMP) is characterized by crustal peraluminous magmas, minor mantle-derived products, and volumetrically significant hybrid products[23]. Magmatic centers were activated by post-collisional extension, as the crust of the Northern Apennines fold-and-thrust belt was progressively thinned to 20–25 km and heated by asthenosphere upwelling during the eastward roll-back of the subducting Adria Plate[24]. Some of the igneous complexes are characterized by a simple intrusive history, while multiple batches of crustal, mantle and hybrid magmas were emplaced in western-central Elba Island (8.4–6.9 Ma), Campiglia Marittima (5.4–4.4 Ma) and Larderello (3.8–1.6 Ma)[13,25].

The Campiglia Marittima igneous complex (Fig. 1, Supplemental Fig. 1) is made of the Botro ai Marmi granite pluton, several subvolcanic mafic and felsic porphyry dykes, and the rhyolitic volcanic complex of San Vincenzo. The intrusive sequence started with the emplacement of the Botro ai Marmi granite magma into a Jurassic limestone sequence at shallow depth (~0.10–0.15 GPa)[26], producing a N–S elongated thermal aureole[27]. The top of the granite body crops out for as little as ~ 0.1 km^2, with a buried roof extending over ~ 18 km^2[22]. The pluton has peraluminous monzo-syenogranite composition (SiO_2 = 68–72 wt%, Alumina Saturation Index = 1.1–1.3) and is made of a light grey facies with pristine igneous features (minor) and a metasomatized white-pinkish facies (dominant). The primary paragenesis consists of quartz, K-feldspar, plagioclase, biotite, and euhedral cordierite along with accessory apatite, zircon and late-magmatic tourmaline. The metasomatized granite is characterized by replacement of oligoclase and biotite by K-feldspar and phlogopite plus titanite, respectively (Supplemental Fig. 1)[21]. Skarn occur as minor proximal masses[21] and large distal bodies associated with Zn-Pb(-Ag) and Cu-Fe mineralizations[27].

The Temperino mafic porphyry[27] occurs as small-volume, isolated dykelets emplaced into distal skarn bodies. The porphyry consists of phenocrysts of plagioclase, biotite, clinopyroxene, orthopyroxene and olivine, commonly replaced by actinolite, epidote, chlorite and carbonates, along with a significant xenocryst cargo of coarse-grained sanidine and quartz, all set in a fine-grained groundmass completely recrystallized to K-feldspar, quartz and chlorite. Accessory minerals are chromite, apatite, zircon, monazite, and ilmenite (Supplemental Fig. 1).

The felsic porphyry dykes are found as three main lithological types[27,28]. The Coquand porphyry consists of two dykes, ~ 2 km-long, and carrying dm-sized mafic enclaves. The Ortaccio porphyry consists of a ~ 8 km-long dyke crosscutting the Coquand dykes and is characterized by abundant cm-sized K-feldspar phenocrysts and scattered small mafic enclaves. The Monticino porphyry is K-feldspar-phyric.

The San Vincenzo rhyolite covers ~ 10 km^2 as viscous lava flows/domes with a mean thickness around 100 m, for a total preserved volume of about 1 km^3. Petrographic[29] and geochemical-isotopic features distinguish the rhyolites into two types[30]. Type-A has vitrophyric texture hosting phenocrysts of quartz, sanidine, plagioclase, biotite, euhedral cordierite, along with accessory apatite, monazite, zircon and ilmenite. Type-B rhyolite is distinguished for the occurrence of fine-grained enclaves of latite composition, scattered ortho- and clinopyroxene xenocrysts, and lower Sr and higher Mg contents with respect to Type-A.

The igneous units of the Campiglia complex cover the whole range of Sr–Nd isotope systematics of the Tuscan Magmatic Province (Supplemental Table 1, Fig. 2). Therefore, they have significantly variable petrological and geochemical origins, ranging from crustal magmas to mantle-derived magmas with hybrid magmas in between.

The Botro ai Marmi granite samples have the highest $^{87}Sr/^{86}Sr_t$ (0.72555–0.72643) and the lowest $^{143}Nd/^{144}Nd_t$ (0.51206–0.512123) of the whole Tuscan Magmatic Province (Supplemental Table 1, Fig. 2).

The Type-A San Vincenzo rhyolites have very high and variable $^{87}Sr/^{86}Sr_t$ (0.71900–0.72507) and low $^{143}Nd/^{144}Nd_t$ (0.51212–0.51222) reaching with some samples the extreme values of the Botro ai Marmi pluton, being therefore close representatives of crust-derived magmas, as well as the Botro ai Marmi granite (Supplemental Table 1, Fig. 2)[24,30]. The Type-B San Vincenzo rhyolites have moderate and variable $^{87}Sr/^{86}Sr_t$ (0.71312–0.71538) and $^{143}Nd/^{144}Nd_t$ (0.51221–0.51224), shifted towards mantle end-members with respect to the Type-A rhyolite[24,30]. On the other hand, the latite enclaves in San Vincenzo rhyolites have the lowermost $^{87}Sr/^{86}Sr_t$ (0.70790–0.70918) and the highest $^{143}Nd/^{144}Nd_t$ (0.51236–0.512520) of the whole Tuscan Magmatic Province, thus representing the composition closest to a mantle end-member[24].

The Temperino porphyry has $^{87}Sr/^{86}Sr_t$ (0.71002–0.71068) and $^{143}Nd/^{144}Nd_t$ (0.51221–0.51222) close to the mantle end-member represented by the latitic San Vincenzo enclaves[23,24].

This variety of igneous rocks, covering the whole geochemical range of the TMP, crop out in a restricted area, with intrusive, subvolcanic and volcanic rocks. This serendipitous geological setting was generated thanks to the quick exhumation of the very young Botro ai Marmi pluton following the eastward lateral extrusion of its carbonate overburden rheologically weakened by thermal metamorphism[22]. Distal skarn and subvolcanic porphyries were emplaced to the east of the pluton, while volcanic rocks were emplaced west of the pluton, in a crustal section not significantly affected by exhumation (Fig. 1).

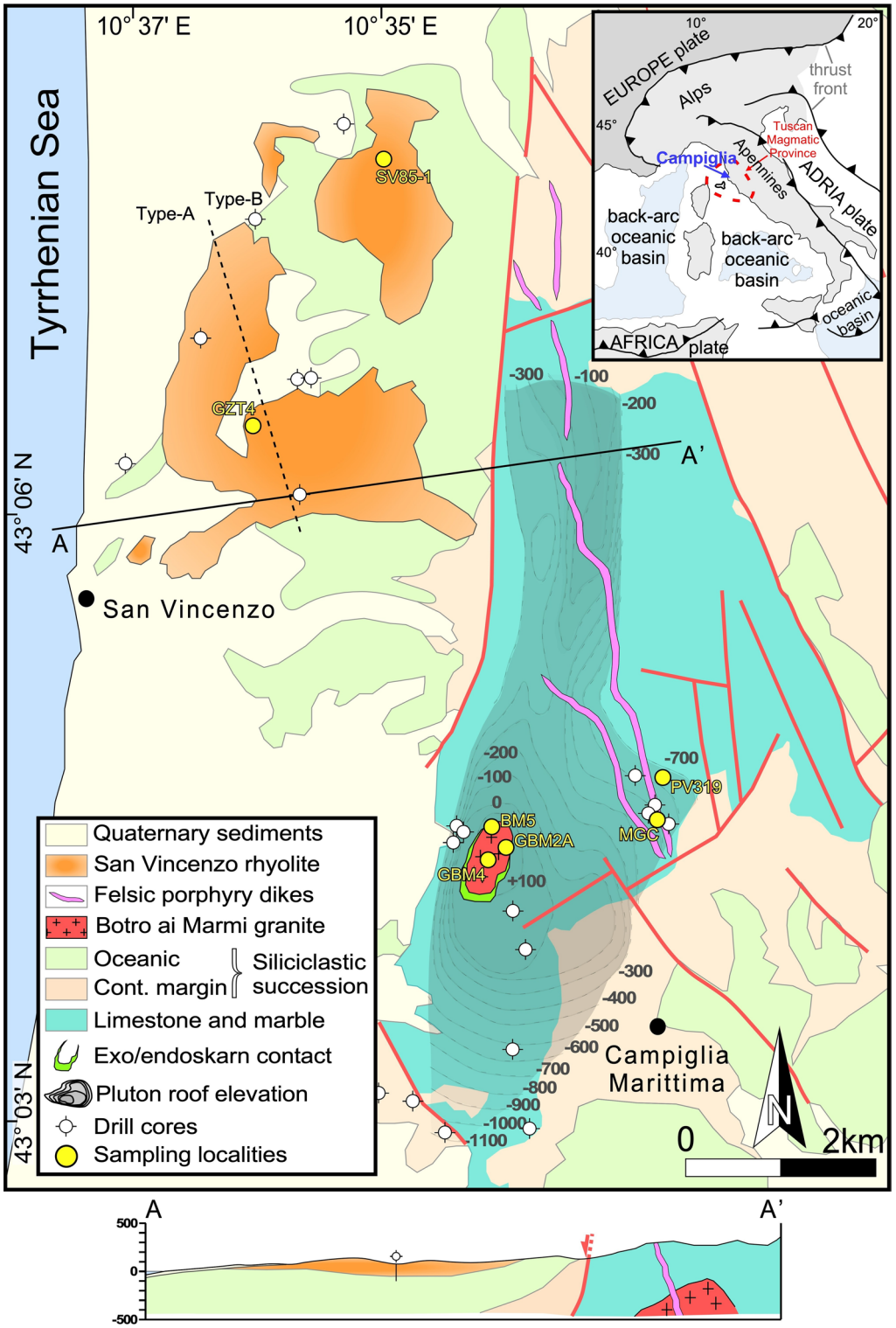

Fig. 1. (**a**) Schematic geological map[27,31] and pluton roof elevation[22] with location of studied samples. (**b**) Schematic geological cross-section, showing the differential exhumation of the eastern block of the Campiglia system, carrying the plutonic-subvolcanic rocks at the same level of the volcanic rock.

Zircon crystallization ages

In total, 59 zircon crystals from 7 samples have been dated by CA-ID-TIMS. All the zircons show simple to oscillatory growth zoning (Fig. 3), typical of an igneous origin.

For the Botro ai Marmi monzogranite, 13 zircon crystals were dated, 4 from each of the two samples of cordierite-biotite granite (BM5 and GBM4), and 5 from the phlogopite-titanite granite (GBM2A; Supplemental

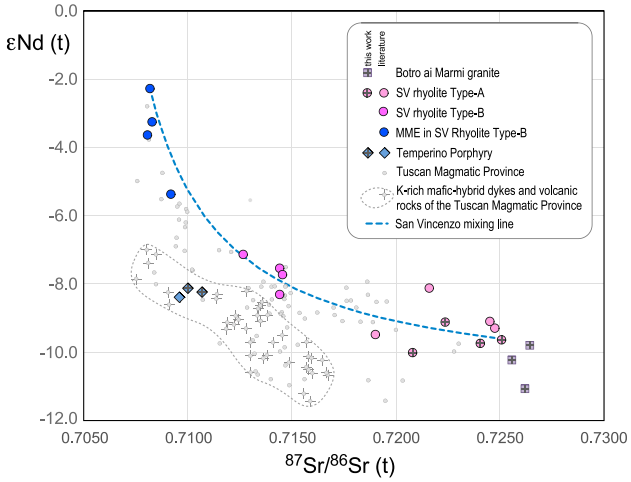

Fig. 2. eNd (t) vs $^{87}Sr/^{86}Sr$ (t) showing the extreme isotopic variability recorded by the Campiglia igneous complex, that covers the whole variability of the Tuscan Magmatic Province. San Vincenzo Type-A and Type-B rhyolites, despite their very similar major element compositions, are characterized by isotopic lying on a mixing curve between the mafic microgranular enclaves (MME) of the San Vincenzo Rhyolites and San Vincenzo Type-A Rhyolites. The hybrid mantle-derived Temperino porphyry plot in the field of mafic-hybrid dykes and volcanic rocks of the TMP (Montecristo porphyritic dykes, Elba Orano porphyry dykes, Capraia latites-shoshonites, Radicofani lavas, Mt Cimino lavas, Mt Amiata lavas, Orciatico-Montecatini lamproites). Some data from Campiglia and data from the rest of the Tuscan Magmatic Province are from literature[24,30–40].

Table 2, Fig. 3). The two samples from pristine to slightly metasomatized cordierite-biotite granite and the sample from the metasomatized phlogopite-titanite granite all have overlapping $^{206}Pb/^{238}U$ zircon dates. This overlap demonstrated that the metasomatic processes, deeply modifying the petrographic/chemical features of the granite[21,41], were not able to affect zircon composition. Overall, $^{206}Pb/^{238}U$ dates range between 5.511 ± 0.063 and 5.404 ± 0.085 Ma, with a total age range covered by zircons from the same unit (excluding the xenocrystic or xenocryst-cored zircons) ΔT_h[42] = 107 ± 106 ka (Fig. 3). The emplacement age of the granite is interpreted as linked to the date of the youngest zircon (5.404 ± 0.085 Ma), resulting identical to the 5.409 ± 0.043 Ma ^{40}Ar-^{39}Ar age for biotite from BM5 sample[28].

For the mafic Temperino porphyry, 10 zircons were dated from two samples (PV319 and MGC; Fig. 3). Overall, $^{206}Pb/^{238}U$ dates range between 5.520 ± 0.11 and 5.068 ± 0.060 Ma, with a total spread ΔT_h = 0.452 ± 0.125 Ma. The youngest zircon date (5.068 ± 0.060) is interpreted as the age of porphyry emplacement, as supported by the overlap with the biotite ^{40}Ar-^{39}Ar age of 5.084 ± 0.027 (Fig. 3)[28].

For the San Vincenzo Type-A rhyolite (sample GZT4), 25 zircon crystals have been dated. They show a total age range ΔT_h = 0.564 ± 0.213 Ma, between 5.60 ± 0.21 and 5.036 ± 0.034 Ma, so that the zircon age dispersion is somewhat larger than observed for the mafic porphyry and much larger than the granite. The youngest zircon date (4.953 ± 0.020 Ma) overlaps within the error of the sanidine ^{40}Ar-^{39}Ar age of 5.0024 ± 0.0062 Ma[28] and is interpreted as the eruption age.

For the Type-B rhyolite (sample SV85-1), 11 zircon crystals have been dated, showing a total range of crystallization ages ΔT_h = 0.388 ± 0.008 Ma, between 4.8682 ± 0.0041 and 4.4802 ± 0.0063 Ma (Fig. 3). The youngest zircon gives a date 4.4802 ± 0.0063 Ma, very close to the sanidine ^{40}Ar-^{39}Ar dates of 4.41 ± 0.04[43], and the more precise 4.4359 ± 0.0045 Ma[28], the latter interpreted as the eruption age.

Crystals significantly older than the main age group are overall rare (4 of 59 dated zircons; Fig. 3). One has been found in Temperino porphyry PV319 (7.369 ± 0.088 Ma), two in the San Vincenzo Type-A rhyolite (6.638 ± 0.033 and 9.758 ± 0.034 Ma) and one in Type-B rhyolite (9.750 ± 0.030 Ma, Supplemental Table 2). They could simply be interpreted as xenocrysts, yet xenocrystic, inherited zircons are proven to be very rare in San Vincenzo lavas and throughout the whole crustal magmas of the TMP[13,44]. Indeed, a LA-HR-ICP-MS screening aimed to look for old xenocryst cores in the most crustal-like igneous rocks of the TMP, including San Vincenzo rhyolite, yielded a surprisingly low number of Paleozoic or older ages of 21 out of 750 data, and, as expected, no cores of Miocene to Triassic age[44]. It is therefore most likely that these few ages represent averaged values between small-volume pre-Mesozoic, inherited cores and volumetrically dominant mantle-rim young autocrystic portions[42], reported as "xenocryst-cored zircons" in (Fig. 3).

Origin of zircon age dispersions

The magmatic-hydrothermal system is a prime case study to investigate timescales in an ore-forming process triggered by igneous plumbing system, owing to its very young age leading to very small errors on high-precision CA-ID-TIMS dates, coupled with exposures of the full range of emplacement levels.

For each igneous unit, the zircon dates cover a range of ages, with two relevant common features. (1) The ages of the oldest zircons (~ 5.52 Ma) are shared by the peraluminous Botro ai Marmi pluton, the mafic Temperino

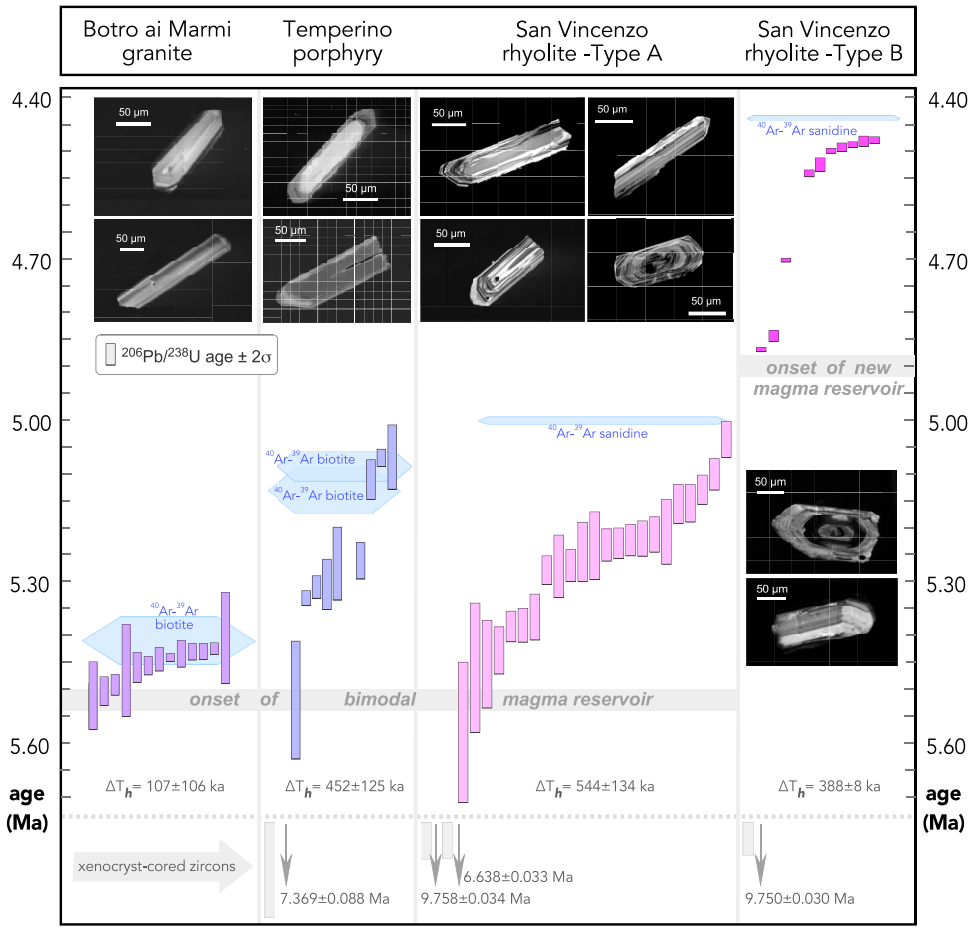

Fig. 3. Geochronological framework for the igneous complex, with zircon CA-ID-TIMS $^{206}Pb/^{238}U$ dates corrected for Th/U disequilibrium (Supplemental Table 2, integrated with biotite and sanidine ^{40}Ar-^{39}Ar dates[28].

porphyry, and the peraluminous San Vincenzo Type-A rhyolite: we infer this is the age of feeding and onset of the deepest part of the plumbing system, with both a felsic, crustal magma reservoir and a mafic-intermediate, mantle-derived magma reservoir. (2) The youngest zircon dates for each unit essentially coincide with sanidine or biotite ^{40}Ar-^{39}Ar ages for the same unit[28]: we interpret this age as the emplacement/eruption age.

On the other hand, the system is characterized by significantly different zircon age dispersions when different igneous episodes are compared to each other.

Botro ai Marmi pluton—All the samples have zircon dates overlapping within each hand sample and across hand samples, and no antecrysts are found. At this initial stage, the plumbing system has no zircons acquired from previous magmatic pulses. The youngest zircon ages overlap the biotite ^{40}Ar-^{39}Ar age and are interpreted as the emplacement age.

Temperino mafic porphyry—The two hand samples yield different zircon crystallization time span, each one of them terminated by slightly younger biotite ^{40}Ar-^{39}Ar age. This is interpreted as evidence for multiple extraction events. Furthermore, the oldest zircon date overlaps the oldest Botro ai Marmi pluton's dates. These latter zircons are interpreted as antecrysts deriving from the plumbing system which was established at ~ 5.5 Ma. This antecrystic origin is supported by the occurrence in the porphyry of sanidine and quartz xenocrysts from a felsic magma/mush. On the other hand, the occurrence of a hidden mantle-derived magma pool into the crust (that in late Miocene was already < 25 km thick) is also supported by (i) metasomatic input of Mg, Ba, Sr into the pluton from a coeval mafic source, (ii) mantle signature of mineralizing fluids, and (iii) extra-heat source to produce the high temperature metamorphism and metasomatism of the pluton carbonate host[21,41].

San Vincenzo Type-A rhyolite—Zircon ages show a significant dispersion of 544 ± 134 ka, covering the whole range shown by the two Temperino samples. For a similar dispersion range in a middle crust intrusion, an exhaustive discussion of the main possible interpretations[42] shed light on the difficulties of choosing among possible interpretations in the case of that intrusion. On the other hand, for San Vincenzo rhyolite, three special features give tight constraints on the interpretation of the age dispersion: (i) the volcanic nature of the studied material, (ii) the availability of a precise sanidine ^{40}Ar–^{39}Ar age coincident with the youngest zircon date and interpreted as the eruption age[28], in agreement with inferences for other large-volume eruptions, where the time span of zircon crystallization terminates with the eruption event dated by sanidine ^{40}Ar–^{39}Ar[11,15,45], and (iii)

the dispersion of zircon dates between the eruption age (5.0 Ma) and the age of the oldest zircons of the system, inferred to represent the age of the establishment of the plumbing system (~5.5 Ma). Thus, these oldest zircons are envisaged as deriving from such a reservoir, fed by crustal and mantle magmas. It is to note that, in this case study, naming them cognate xenocrysts or antecrysts or autocrysts is of minor significance, owing to the crust-mantle double nature of the feeding system.

San Vincenzo Type-B rhyolite—Zircon ages split into two groups: the youngest zircon of the youngest cluster has an age -almost- overlapping the sanidine ^{40}Ar–^{39}Ar age that, as for Type-A rhyolite, is interpreted as the eruption age[28]; zircons from the oldest group are distinctly older, yet significantly younger than the eruption age of Type-A rhyolite. Thus, all the zircons are significantly younger than the eruption age of the Type-A rhyolite: the youngest eruption did not cannibalize any older zircon from the felsic-mafic reservoir. The zircons from Type-B rhyolite appear to have crystallized in a system with no memory of the previous plumbing system. So, we believe that another deep reservoir was active between 5.00 and 4.45 Ma as inferred by the significant petrological difference between Type-A and Type-B rhyolites, i.e., the stark evidence for mingling-mixing between crustal and mantle magma in the pre-eruptive system in later, Type-B rhyolite which actually represents a hybrid melt.

Interplay between magma feeding, extraction and ore genesis

The extended, ~500 ka, crystallization ages of the two rhyolite types, with no zircon age overlap between them, points out two separate igneous cycles. Both cycles were fed by felsic and mafic magmas in their earliest stages, but they nevertheless evolved in different ways. The first cycle (~5.5–5.0 Ma) is characterized by separate, independent emplacement of felsic magmas, mafic magma, and mineralizing fluids, with no evidence for chemical interaction between the two types of magmas. The second cycle is characterized by mingling in every emplacement episode, witnessed by the occurrence of mafic microgranular enclaves (MME) in felsic dykes and MME plus mafic xenocrysts in the Type-B rhyolite. Additionally, no evidence for activity of mineralizing fluids is found in the second cycle.

Thus, a history of asynchronous interplay between magma feeding, magma extraction, magma emplacement/eruption and activity of mineralizing fluids can be outlined (Fig. 4). The first felsic feeding event occurred at 5.52 Ma, when the oldest zircons started to crystallize. This magma batch did activate a mid-crustal reservoir, that soon gave way to the emplacement in the shallow crust of Botro ai Marmi peraluminous magma at 5.44 Ma. The 5.38 Ma development of Mg- and Fe-rich exoskarn [28], proximal to the Botro ai Marmi pluton, is interpreted as evidence for arrival in the deep reservoir of a mafic magma batch[21,27,41], setting up a bimodal reservoir from which the Fe–Mg metasomatic fluids are issued. The genesis of Zn-Pb-Ag ores between 5.38 and 5.1 Ma[28] is related to the release of another batch of mineralizing fluids[27]. The age could be inferred to be at ~5.23 Ma, coincident with the second-rank peak in the abundance of zircon dates, indicating a pulse in crystallization inducing release of mineralizing fluids. The genesis of Fe-Cu ore, overprinting the previous Zn-Pb-Ag ores (reverse telescoping process)[27], is linked to hot mafic fluids and to the minor volume of mafic Temperino Porphyry magma as well, issuing from mafic magma in the deep reservoir. This episode is inferred to coincide with the third-rank peak in zircon age distribution, around 5.24 Ma (Fig. 4). The San Vincenzo Type-A rhyolite then erupted at 5.00 Ma from part of the deep reservoir not affected by mass contribution of mafic melt, and nevertheless remained in a partially molten state for more than 500 ka, as indicated by the extended period of zircon crystallization.

560 ka passed before the next eruption of Type-B San Vincenzo rhyolitic hybrid magma at 4.436 Ma. The oldest zircon in this rhyolite is 4.87 Ma, and zircons older than 5 Ma are missing at all, suggesting the establishment of a new, independent reservoir. This reservoir likely fed three episodes of emplacement of felsic dykes carrying mafic microgranular enclaves, the Coquand, Ortaccio and Monticino porphyries[27], whose ^{40}Ar-^{39}Ar ages, even affected by some uncertainty, are overlapping with the three secondary peaks of zircon distribution of the Type-B rhyolite at ~4.88, ~4,68 and ~4.50 Ma, respectively. Thus, a new deep bimodal reservoir was established around 4.9 Ma and fed the MME-bearing dykes and, finally, the eruption of Type-B rhyolite. The supply of a new, independent felsic magma batch is also supported by the comparison of chemical and isotopic composition of Type-A and Type-B rhyolites: they have the same overall chemical composition, but significantly different Sr isotopic compositions[30]. Assuming that isotope variabilities are originated by magma mixing, a simple Sr-isotopic modelling would require at least 20 wt% of mafic melt (San Vincenzo MME) in the hybrid system, that would displace the rhyolite to significantly lower SiO_2 content (some 5 wt%), which is not observed. The bulk of this evidence led to infer a new cycle/system, isolated from the first bimodal reservoir, also involving a mafic magma with a Nd isotopic ratio distinctly higher than the earlier mafic magma recorded by the Temperino porphyry (Fig. 2). This is coherent with the post-collisional geodynamic setting, where small volume of magmas are generated and rapidly extracted from a thinned crustal source[46] characterized by extremely high thermal gradients from underlying uplifted mantle.

Conclusions

In summary, for the Campiglia plumbing system, the exposures of the full range of magma emplacement levels, combined with young ages of the products and high precision CA-ID-TIMS geochronology reveal a complex distribution of zircon crystallization ages, spanning over more than 1 Ma. The full distribution of zircon ages can be understood only in the light of the dynamics of the different levels of the reservoirs integrated with the genesis of metasomatic rocks linked to the release of fluids from the plumbing system.

A bimodal deep reservoir, once activated at ~5.5 Ma, for the following ~550 ka remains in magmatic conditions (i.e., melt-present) with the help from the input of mafic, mantle-derived melt. The three events of magma emplacement/eruptions tapped the same reservoir, with common oldest zircon ages and progressively younger youngest zircons. The feeding episodes and release of mineralizing fluids show asynchrony, as revealed by the generation of skarn and/or ore deposits.

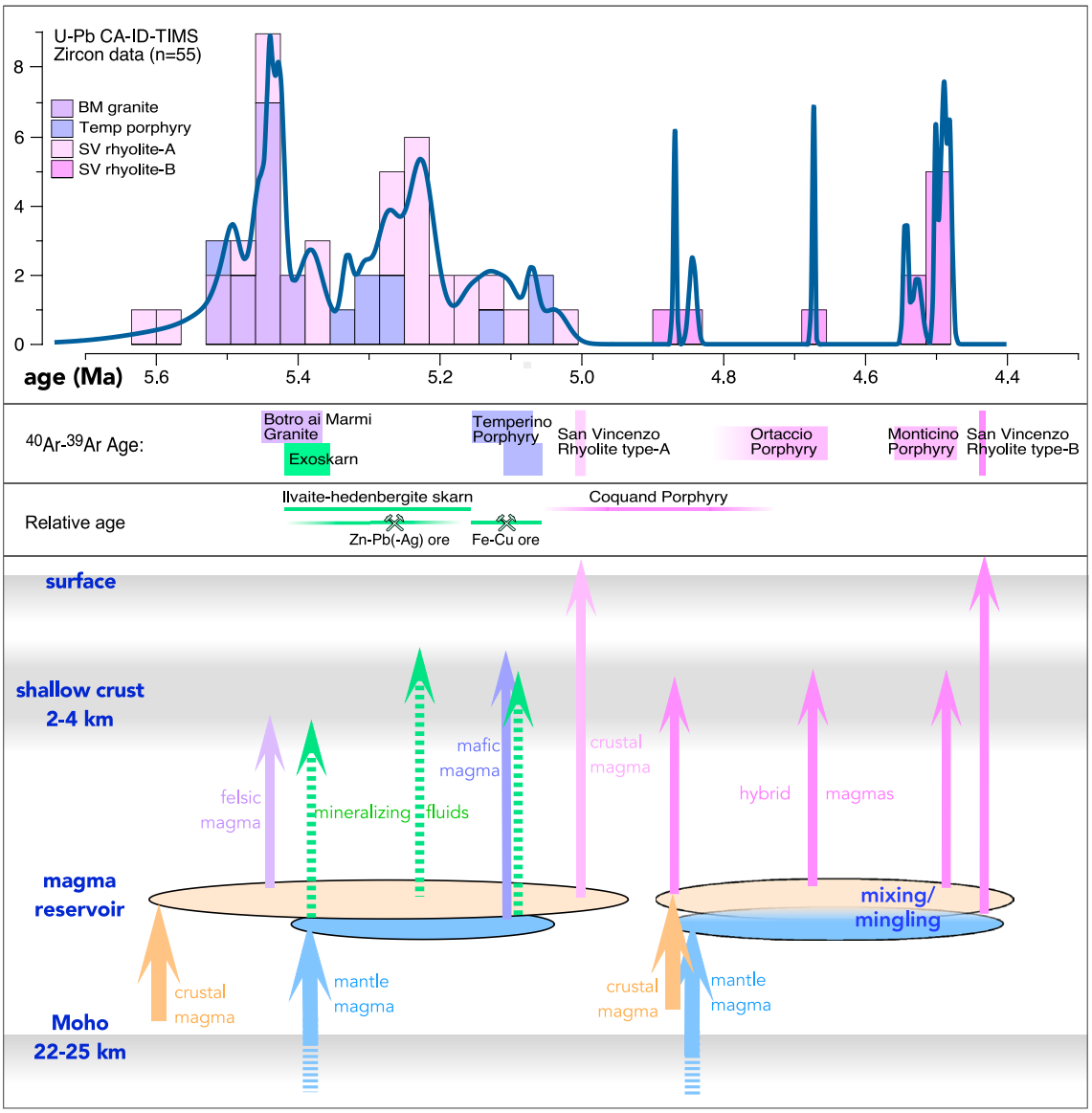

Fig. 4. Scenario for asynchronous transfer of magmas and mineralizing fluids in the Campiglia plutonic-subvolcanic-volcanic plumbing system in relation to the geochronological framework. Continuous arrows: transfer of magma, dashed arrows: transfer of mineralizing fluids.

Another deep reservoir is then established after the first major rhyolite eruption, to feed felsic dykes and a rhyolite eruption, all characterized by mingling processes, but not accompanied by mineralizing fluids. The two main eruption episodes both mark the end of a magmatic cycle lasting some 550 ka, with only the earliest cycle characterized by generation of ore deposits. In the Larderello geothermal area, a similar history is documented, with ore occurrences linked to the oldest igneous cycle, while no ores have been found associated with the youngest intrusions, despite the large numbers of deep wells drilled in the area for geothermal exploration.

The Campiglia system thus reveals an asynchrony between transfer of magmas and ore-forming fluids, as pointed out by isotopic and relative ages of igneous rocks, metasomatic products and ore deposits. Thus, the Campiglia plutonic-subvolcanic-volcanic plumbing system represents a prime case study thanks to the quick and differential exhumation that helps understanding the connection between processes originally occurring at different crustal levels.

Data availability

All data generated or analysed during this study are included in this published article and its supplementary information files.

Received: 21 December 2024; Accepted: 5 September 2025
Published online: 05 December 2025

References

1. Caricchi, L., Simpson, G. & Schaltegger, U. Estimates of volume and magma input in crustal magmatic systems from zircon geochronology: The effect of modeling assumptions and system variables. *Front. Earth Sci.* https://doi.org/10.3389/feart.2016.00048 (2016).
2. Leuthold, J. et al. Time resolved construction of a bimodal laccolith (Torres del Paine, Patagonia). *Earth Planet. Sci. Lett.* **325–326**, 85–92. https://doi.org/10.1016/j.epsl.2012.01.032 (2012).
3. Schaltegger, U., Schmitt, A. K. & Horstwood, M. S. A. U–Th–Pb zircon geochronology by ID-TIMS, SIMS, and laser ablation ICP-MS: recipes, interpretations, and opportunities. *Chem. Geol.* **402**, 89–110. https://doi.org/10.1016/j.chemgeo.2015.02.028 (2015).
4. Barboni, M. & Schoene, B. Short eruption window revealed by absolute crystal growth rates in a granitic magma. *Nature Geosci* **7**, 524–528. https://doi.org/10.1038/ngeo2185 (2014).
5. Casalini, M. et al. Geochemical and radiogenic isotope probes of Ischia volcano, Southern Italy: Constraints on magma chamber dynamics and residence time. *Amer. Mineral.* **102**, 262–274. https://doi.org/10.2138/am-2017-5724 (2017).
6. Wotzlaw, J. F. et al. Tracking the evolution of large-volume silicic magma reservoirs from assembly to supereruption. *Geology* **41**, 867–870. https://doi.org/10.1130/g34366.1 (2013).
7. Menand, T., de Saint-Blanquat, M. & Annen, C. Emplacement of magma pulses and growth of magma bodies. *Tectonophys.* **500**, 1–2 (2011).
8. Caricchi, L., Simpson, G. & Schaltegger, U. Zircons reveal magma fluxes in the Earth/'s crust. *Nature* **511**, 457–461. https://doi.org/10.1038/nature13532 (2014).
9. Miller, J. S., Matzel, J. E. P., Miller, C. F., Burgess, S. D. & Miller, R. B. Zircon growth and recycling during the assembly of large, composite arc plutons. *J. Volcanol. Geoth. Res.* **167**, 282–299 (2007).
10. Cashman, K. V. & Giordano, G. Calderas and magma reservoirs. *J. Volcanol. Geoth. Res.* **288**, 28–45. https://doi.org/10.1016/j.jvolgeores.2014.09.007 (2014).
11. Deering, C. D. et al. Zircon record of the plutonic-volcanic connection and protracted rhyolite melt evolution. *Geology* https://doi.org/10.1130/G37539.1 (2016).
12. Stelten, M. E., Cooper, K. M., Vazquez, J. A., Calvert, A. T. & Glessner, J. J. G. Mechanisms and timescales of generating eruptible rhyolitic magmas at yellowstone caldera from zircon and sanidine geochronology and geochemistry. *J. Petrol.* **56**, 1607–1642. https://doi.org/10.1093/petrology/egv047 (2015).
13. Farina, F. et al. Zircon petrochronology reveals the timescale and mechanism of anatectic magma formation. *Earth Planet. Sci. Lett.* **495**, 213–223. https://doi.org/10.1016/j.epsl.2018.05.021 (2018).
14. Curry, A. et al. Timescales and thermal evolution of large silicic magma reservoirs during an ignimbrite flare-up: perspectives from zircon. *Contrib. Mineral. Petrol.* https://doi.org/10.1007/s00410-021-01862-w (2021).
15. Bachmann, O., Charlier, B. L. A. & Lowenstern, J. B. Zircon crystallization and recycling in the magma chamber of the rhyolitic Kos Plateau Tuff (Aegean arc). *Geology* **35**, 73–76. https://doi.org/10.1130/g23151a.1 (2007).
16. Payacán, I., Gutiérrez, F., Bachmann, O. & Parada, M. Á. Differentiation of an upper crustal magma reservoir via crystal-melt separation recorded in the San Gabriel pluton, central Chile. *Geosphere* **19**, 348–369. https://doi.org/10.1130/ges02535.1 (2023).
17. Wotzlaw, J. F. et al. Linking rapid magma reservoir assembly and eruption trigger mechanisms at evolved Yellowstone-type supervolcanoes. *Geology* **42**, 807–810. https://doi.org/10.1130/g35979.1 (2014).
18. Large, S. J. E. et al. Copper-mineralised porphyries sample the evolution of a large-volume silicic magma reservoir from rapid assembly to solidification. *Earth Planet. Sci. Lett.* https://doi.org/10.1016/j.epsl.2021.116877 (2021).
19. Large, S. J. E., Wotzlaw, J.-F., Guillong, M., von Quadt, A. & Heinrich, C. A. Resolving the timescales of magmatic and hydrothermal processes associated with porphyry deposit formation using zircon U-Pb petrochronology. *Geochronology* **2**, 209–230. https://doi.org/10.5194/gchron-2-209-2020 (2020).
20. Large, S. J. E. et al. Tectonic and crustal processes drive multi-million year arc magma evolution leading up to porphyry copper deposit formation in Central Chile. *J. Petrol.* https://doi.org/10.1093/petrology/egae023 (2024).
21. Paoli, G., Dini, A. & Rocchi, S. Footprints of element mobility during metasomatism linked to a late Miocene peraluminous granite intruding a carbonate host (Campiglia Marittima, Tuscany). *Int. J. Earth Sci.* **108**, 1617–1641. https://doi.org/10.1007/s00531-019-01723-9 (2019).
22. Vezzoni, S., Rocchi, S. & Dini, A. Lateral extrusion of a thermally weakened pluton overburden (Campiglia Marittima, Tuscany). *Int. J. Earth Sci.* https://doi.org/10.1007/s00531-017-1539-9 (2018).
23. Poli, G. & Peccerillo, A. The Upper Miocene magmatism of the Island of Elba (Central Italy): compositional characteristics, petrogenesis and implications for the origin of the Tuscany Magmatic Province. *Mineral. Petrol.* https://doi.org/10.1007/s00710-016-0426-6 (2016).
24. Dini, A., Innocenti, F., Rocchi, S., Tonarini, S. & Westerman, D. S. The magmatic evolution of the laccolith-pluton-dyke complex of Elba Island, Italy. *Geol. Mag.* **139**, 257–279 (2002).
25. Dini, A., Gianelli, G., Puxeddu, M. & Ruggieri, C. Origin and evolution of Pliocene-Pleistocene granites from the Larderello geothermal field (Tuscan Magmatic Province, Italy). *Lithos* **81**, 1–31 (2005).
26. Leoni, L. & Tamponi, M. Thermometamorphism in the Campiglia Marittima aureole. *Neues Jahrbuch Miner. Mh.* **1991**, 145–157 (1991).
27. Vezzoni, S., Dini, A. & Rocchi, S. Reverse telescoping in a distal skarn system (Campiglia Marittima, Italy). *Ore Geol. Rev.* **77**, 176–193. https://doi.org/10.1016/j.oregeorev.2016.03.001 (2016).
28. Di Vincenzo, G., Vezzoni, S., Dini, A. & Rocchi, S. Timescale of a magmatic-hydrothermal system revealed by 40Ar–39Ar geochronology: the Mio-Pliocene Campiglia Marittima system (Tuscany, Italy). *Sci. Rep.* https://doi.org/10.1038/s41598-022-10867-9 (2022).
29. Ridolfi, F. et al. Unravelling the complex interaction between mantle and crustal magmas encoded in the lavas of San Vincenzo (Tuscany, Italy). *Part I: Petrogr. Thermobaromet. Lithos* **244**, 218–232. https://doi.org/10.1016/j.lithos.2015.09.029 (2016).
30. Ferrara, G., Petrini, R., Serri, G. & Tonarini, S. Petrology and isotope geochemistry of San Vincenzo rhyolites (Tuscany, Italy). *Bull. Volc.* **51**, 379–388 (1989).
31. Pinarelli, L., Poli, G. & Santo, A. P. Geochemical characterization of recent volcanism from the Tuscan magmatic province (Central Italy): the Roccastrada and San Vincenzo centers. *Periodico di Mineral.* **58**, 67–96 (1989).
32. Conticelli, S. et al. Shoshonite and sub-alkaline magmas from an ultrapotassic volcano: Sr–Nd–Pb isotope data on the Roccamonfina volcanic rocks, Roman Magmatic Province, Southern Italy. *Contrib. Mineral. Petrol.* **157**, 41–63 (2009).
33. Conticelli, S., Avanzinelli, R., Marchionni, S., Tommasini, S. & Melluso, L. Sr-Nd-Pb isotopes from the Radicofani Volcano, Central Italy: constraints on heterogeneities in a veined mantle responsible for the shift from ultrapotassic shoshonite to basaltic andesite magmas in a post-collisional setting. *Mineral. Petrol.* **103**, 123–148. https://doi.org/10.1007/s00710-011-0161-y (2011).
34. Juteau, M., Michard, A., Zimmermann, J.-L. & Albarede, F. Isotopic heterogeneities in the granitic intrusion of Monte Capanne (Elba Island, Italy) and dating concepts. *J. Petrol.* **25**, 532–545 (1984).
35. Juteau, M., Michard, A. & Albarede, F. The Pb-Sr-Nd isotope geochemistry of some recent circum-Mediterranean granites. *Contrib. Mineral. Petrol.* **92**, 331–341 (1986).
36. Westerman, D. S., Innocenti, F., Tonarini, S. & Ferrara, G. The Pliocene intrusions of the Island of Giglio (Tuscany). *Mem. Soc. Geol. It.* **49**, 345–363 (1993).
37. Innocenti, F., Westerman, D. S., Rocchi, S. & Tonarini, S. The Montecristo monzogranite (Northern Tyrrhenian Sea, Italy): a collisional pluton in an extensional setting. *Geol. J.* **32**, 131–151 (1997).

38. Hawkesworth, C. J. & Vollmer, R. Crustal contamination versus enriched mantle 143Nd/144Nd and 87Sr/86Sr evidence from the Italian Volcanics. *Contribut. Mineral. Petrol.* **69**, 151–165 (1979).
39. Poli, G., Frey, F. A. & Ferrara, G. Geochemical characteristics of the South Tuscany (Italy) volcanic province: constraints on lava petrogenesis. *Chem. Geol.* **43**, 203–221 (1984).
40. D'Orazio, M., Serri, G., Innocenti, F. & Petrini, R. Il vulcano di Radicofani nel quadro del magmatismo neogenico-quaternario dell'Appennino settentrionale. *Stud. Geol. Camerti* **199**, 79–92 (1994).
41. Paoli, D. & Petrelli, R. HFSE-REE transfer mechanisms during metasomatism of a late miocene peraluminous granite intruding a carbonate host (Campiglia Marittima, Tuscany). *Minerals* https://doi.org/10.3390/min9110682 (2019).
42. Samperton, K. M. et al. Magma emplacement, differentiation and cooling in the middle crust: Integrated zircon geochronological–geochemical constraints from the Bergell Intrusion, Central Alps. *Chem. Geol.* **417**, 322–340. https://doi.org/10.1016/j.chemgeo.2015.10.024 (2015).
43. Feldstein, S. N., Halliday, A. N., Davies, G. R. & Hall, C. M. Isotope and chemical microsampling: Constraints on the history of an S-type rhyolite, San Vincenzo, Tuscany, Italy. *Geochim. Cosmochim. Acta* **58**, 943–958 (1994).
44. Paoli, G. *Gli zirconi dei magmi crostali della Provincia Magmatica Toscana: morfologie ed età U-Pb* MSci Thesis thesis, (Università di Pisa, 2013).
45. Bachmann, O. et al. 40Ar/39Ar and U–Pb dating of the fish canyon magmatic system, San Juan Volcanic field, Colorado: Evidence for an extended crystallization history. *Chem. Geol.* **236**, 134–166 (2007).
46. Farina, F., Dini, A., Rocchi, S. & Stevens, G. Extreme mineral-scale Sr isotope heterogeneity in granites by disequilibrium melting of the crust. *Earth Planet. Sci. Lett.* **399**, 103–115. https://doi.org/10.1016/j.epsl.2014.05.018 (2014).

Acknowledgements

This work is part of the Ph.D. project of GP at the University of Pisa and was supported by the University of Pisa research projects PRA_2018_19, PRA_2022_66, the MUR project TEOREM prot. 2017AK8C32, and by the Istituto di Geoscienze e Georisorse-CNR (EU-H2020 DESCRAMBLE Project 640573). We express our gratitude to two anonymous reviewers whose comments have strengthened the original version of the manuscript, and to CR for her additional comments and suggestions. Part of this research was funded by the National Plan of Recovery and Resilience (PNRR), funded by the European Union– Next Generation EU, Mission 4, Component C2, Investment 1.1 CUP B53D23034210001, Project PRIN 2022 PNRR - MOLIERE (P20224492Z) - "The antimony resource in Italy: evaluation of environmental impact and ore exploration of a critical raw material".

Author contributions

G.P., A.D., S.V. and S.R. wrote the main manuscript text which all authors reviewed and commented on; S.V. and S.R. prepared Figs. 1–4; all authors prepared the supplemental material; M.O., A.D. and G.P. collect data; all authors analysed the data and discussed the results.

Declarations

Competing interests

The authors declare no competing interests.

Additional information

Supplementary Information The online version contains supplementary material available at https://doi.org/10.1038/s41598-025-19201-5.

Correspondence and requests for materials should be addressed to G.P. or S.V.